Advanced Powder Technology 33 (2022) 103732

Contents lists available at ScienceDirect

Advanced Powder Technology

journal homepage: www.elsevier.com/locate/apt

Original Research Paper

In situ discovery on the formation of supported silver catalysts for ethylene epoxidation ☆

Like Sun [a,b], Haoyang Huang [b,c], Ping Che [a,*], Qiang Lin [d], Kuo Lian [d], Jinbing Li [d], Yu Zhang [b,c], Yongsheng Han [b,c,*]

[a] School of Chemistry and Biological Engineering, University of Science & Technology Beijing, 100083, China
[b] State Key Laboratory of Multiphase Complex Systems, Institute of Process Engineering, Chinese Academy of Sciences, Beijing 100190, China
[c] School of Chemical Engineering, University of Chinese Academy of Science, Beijing 100049, China
[d] Beijing Research Institute of Chemical Industry, Yanshan Branch, SINOPEC, Beijing 102500, China

ARTICLE INFO

Article history:
Received 5 February 2022
Received in revised form 17 June 2022
Accepted 22 June 2022
Available online 5 August 2022

Keywords:
Silver catalysts
Thermal decomposition
Ethylene epoxidation
Selectivity
Size effect

ABSTRACT

Silver particles supported on alumina are the main industrial catalysts for ethylene epoxidation. Silver catalysts are usually produced by an impregnation method followed by thermal decomposition. Although the decomposition process determines the structures and properties of silver catalysts, we are short of information on this high temperature process. Herein we employed a confocal laser scanning microscope (CLSM) equipped with a heating stage to disclose the thermal decomposition process of silver precursor towards the preparation of high selective silver catalysts. It is found that the formation of silver catalysts experiences two steps: crystallization and decomposition. The crystallization occurs at the temperature below 80℃, resulting in the formation of silver complex. Further heating the sample to 140℃, leads to the formation of silver particles at alumina wafers. The atmosphere has a significant effect on the formation and performance of catalysts. When the samples are heated in the nitrogen, small silver particles with similar size are formed, which leads to a high selectivity of ethylene epoxidation. The role of thermal atmospheres on the size and property of silver catalysts is discussed in this paper.

1. Introduction

Silver is the industrial catalyst of the epoxidation of ethylene to produce ethylene oxide (EO) [1,2]. The main consumption of EO is to generate ethylene glycol (EG). EG is an important chemical raw material to produce antifreezing agents and plastics such as polyethylene terephthalate (PET) [3,4]. EG is also a common solvent in the pharmaceutical industry. Silver catalysts are the key techniques in the production of EO and EG, which attracts great interest of industrial and scientific communities. In the competition of developing silver catalyst, selectivity is the most important index for silver catalysts since the ethylene oxidation is prone to produce the by-product of carbon dioxide [5–7]. Ethylene epoxidation is accompanied by two highly thermodynamically favored side reactions: total combustion of ethylene and total combustion of ethylene oxide to form the by-product of carbon dioxide, as shown in the following chemical formulations (1)-(3). These two side reactions (2) and (3) present great challenges for catalysts to reach high selectivity.

$$C_2H_4 + \frac{1}{2}O_2 \rightarrow C_2H_4O \Delta H = -105 kJ/mol \quad (1)$$

$$C_2H_4 + 3O_2 \rightarrow 2CO_2 + 2H_2O \Delta H = -1327 kJ/mol \quad (2)$$

$$C_2H_4O + \frac{5}{2}O_2 \rightarrow 2CO_2 + 2H_2O \Delta H = -1223 kJ/mol \quad (3)$$

Great efforts have been devoted to developing silver catalysts with high selectivity [8–11]. Among them, the effects of size and morphology of catalysts were extensively investigated. Different morphologies of catalysts led to different crystal facets exposed [12–14], resulting in diverse performance of silver catalysts. For example, Christopher synthesized silver nanowires and silver nanocubes with mostly exposed (100) facet by polyol method which has shown excellent selectivity [15,16]. However, silver nanowires and silver nanocubes suffered from structure degradation and selectivity reduction in long-term catalytic processes [17].

☆ Open Access for this article was sponsored by the Society of Powder Technology, Japan, through the KAKENHI Grant Number 18HP2009/Grant-in-Aid for Publication of Scientific Research Results, Japan Society for the Promotion of Science, 2022/2023.
* Corresponding authors.
E-mail addresses: cheping@ustb.edu.cn (P. Che), yshan@ipe.ac.cn (Y. Han).

https://doi.org/10.1016/j.apt.2022.103732

The size effect of silver catalysts was also investigated and different opinions were proposed [18–21]. Some groups reported that the selectivity of silver catalysts was dependent on their size [22–24]. For example, Verykios observed a minimal complete oxidation rate for ethylene epoxidation in a specific size ranging from 50 to 70 nm [25]. However, Bukhtiyarov reported that large silver catalysts showed an improved selectivity since the catalytic active sites of anionic oxygen species were largely formed on lager particles but not on small particles by using X-ray photoelectron spectroscopy (XPS) [26]. He attributed the size effect to the different electronic states of silver atoms at the surface of particles. Besides, Van den Reijen reported that the selectivity of silver catalysts was independent on particle size when the measurements were conducted at the constant conversion of ethylene [27]. These conflicting points on the size effect of silver catalysts attracted our attention to conduct this study, with special interest to reveal the formation process of silver catalysts and to develop a facile strategy to control the size of silver particles.

Silver catalysts were usually prepared by the impregnation method which involves the impregnation of alumina support into silver solution, followed by drying and heating. It was reported that the thermal atmosphere has a significant effect on the size of particles supported. Sun studied the effect of atmosphere on the activity and selectivity of cobalt loaded on zeolites sieves for Fischer-Tropsch reaction which refers that CO and H_2 are catalytically converted into hydrocarbons via surface polymerization [28]. They found that the dispersibility of cobalt particles was improved in the zeolites sieves when the catalysts were pretreated in NO atmosphere, so that the catalysts had a better CH_4 selectivity. This finding enlightened us to disclose the atmosphere effect on the property of silver catalysts. A deep understanding of the formation process of silver catalysts may have important scientific and practical significance to develop better silver catalysts.

In this work, we employed CLSM equipped with a heating stage to disclose the thermal decomposition process of silver precursor towards the formation of high selectivity of silver catalysts. The thermal decomposition process was conducted in different atmospheres, including air and nitrogen gas. The silver particles synthesized were characterized by electron microscopy and X-ray diffraction. The silver catalysts were evaluated for ethylene epoxidation. The effect of thermal atmosphere on the size and property of silver catalysts was discussed in this paper.

2. Materials and methods

2.1. Materials

Silver nitrate ($AgNO_3$, 99 %), oxalic acid dihydrate ($C_2H_2O_4{\cdot}2H_2O$, 99 %), ethylenediamine ($C_2H_8N_2$, 99 %), aluminium hydroxide ($Al(OH)_3$, 99 %), pseudo boehmite ($AlOOH{\cdot}nH_2O$, 99 %), magnesium fluoride (MgF_2, 99 %), barium acetate ($C_4H_6O_4{\cdot}Ba$, 99 %) were purchased from Aladdin (Shanghai). Ultra-pure water (with a resistance of more than 18.2 MΩ cm) obtained from a Millipore Milli-Q system was used in all experiments.

2.2. Preparation of silver catalysts

Silver oxalate was used as the silver precursor. Its suspension was prepared by adding a 40 mL, 0.35 M aqueous solution of silver nitrate to 60 mL, 0.35 M aqueous solution of oxalic acid dihydrate at 60 °C, followed by filtrating and washing the precipitate with Milli-Q water. Silver oxalate was dissolved in an aqueous solution containing 34.7 % ethylene diamine giving a solution containing 30 wt% silver. The α-Al_2O_3 was used as the support of catalysts [29]. The morphology of alumina support was shown in Fig. S1. The α-Al_2O_3 was impregnated in the silver solution under vacuum for 10 min. After filtering the α-Al_2O_3 from the impregnated solution, the samples were dried at room temperature and heated in the tube furnace at different atmospheres.

2.3. In-situ observation of the formation of silver catalysts

CLSM (Zeiss 710) equipped with a heating stage (Linkam TS 1500) was employed to observe the in-situ formation of silver catalysts. The impregnated solution was dropped on the α-Al_2O_3 wafer with a thickness of 1 mm. Then the sample was placed on the heating stage. The time interval for taking pictures was set to 12 s, and the heating rate was set to 5 °C/min. The original video exported from the CLSM was at one frame per second. The videos in the supporting information have been accelerated 5 times which was 60 times faster than the actual phenomena.

2.4. Characterizations of silver catalysts

The size and structure of silver catalysts were characterized by a high-resolution transmission electron microscope (HRTEM, JEM-F200) and a scanning electron microscope (SEM, JSM-7800 Prime). Based on the SEM images processed by Image J software, the size distribution of silver particles was calculated. X-ray diffraction (XRD, Empyrean) was operated in the reflection mode with Cu Kα radiation (λ = 0.1524 nm) in the 2θ range of 5° to 90°. The weight loss behavior of samples was recorded by thermogravimetric and differential thermal analysis (TG-DTA, LABYSYS EVO). The sample was heated from 25 °C to 200 °C at a rate of 2 °C/min. The mass spectrometer (MS, Prima BT) was connected to the TG-DTA instrument to monitor the gaseous products produced in the course of heating. The carbon dioxide produced was monitored at m/e = 44, and water at m/e = 18. To disclose the intermediate of thermal decomposition, the impregnated solution was heated in the furnace in air or nitrogen atmosphere at 60 °C for 12 h. The functional groups of crystals collected from the impregnated solution were identified using Fourier transform infrared spectra (FT-IR, NICOLET iS 50) and XPS (ESCALAB 250Xi).

2.5. Catalysts evaluation for ethylene epoxidation

The ethylene epoxidation reaction was evaluated in a stainless steel fixed-bed reactor with an inner diameter of 4 mm, a schematic illustration of the setup was shown in Fig. S2. The silver catalysts supported on alumina were broken and sieved to 0.9–1.4 mm, and loaded into the reactor. The gas feed composition was C_2H_4 28.5 %, O_2 7.5 %, CO_2 1.5 %, ethylene dichloride 0.1 to 0.5 ppm and balance N_2 with 1.8 MPa total pressure, and the gas hourly space velocity was 6000 h^{-1}. The temperature was recorded when the ethylene oxide concentration in the outlet gas stream reached 2 %. The inlet and outlet gas compositions were measured by the MS. The gas concentrations from 10 ppm to 100 % were analyzed by a Stand Faraday detector, and the gas concentrations from 10 ppb to 100 ppm were detected by secondary electron multiplier.

The EO selectivity was measured to evaluate silver catalysts. The EO selectivity is the ratio of ethylene converted to EO ($n_{E,EO}$) to the total converted ethylene (n_E).

$$EO_{sel.} = \frac{n_{E,EO}}{n_E} \times 100\% \quad (4)$$

Where $EO_{sel.}$ is the ethylene oxide selectivity, $n_{E,EO}$ is the amount of ethylene converted to EO, n_E is the amount of total converted ethylene.

$$n_{E,EO} = \Delta EO \times V \quad (5)$$

$$n_E = \Delta EO \times V + 0.5\Delta CO_2 \times V \quad (6)$$

$$EO_{sel.} = \frac{\Delta EO}{\Delta EO + 0.5\Delta CO_2} \times 100\% \quad (7)$$

Where ΔEO is the difference in molar concentration of EO between the outlet and inlet gas; ΔCO_2 is the difference in molar concentration of CO_2 between the outlet and inlet gas; V is the volume of the gas detected by the mass spectrometer. The volumes of gas at the inlet and outlet of the reactor were kept the same.

3. Results and discussion

Silver catalysts supported on the alumina wafer were prepared by thermally decomposing silver precursor at various atmospheres to reveal the effect of thermal atmosphere on the formation of silver particles, as shown in Fig. 1a. Silver catalysts were synthesized by impregnation method, whereby the concentrations of precursor, temperature and gas flow rate were kept the same in all the experiments. Two types of atmospheres were used in this study, namely air and nitrogen. The choice of atmospheres had a consideration on the industrial preparation of silver catalysts, in which feasibility and safety are important issues. When the silver precursor was heated in nitrogen atmospheres, spherical silver particles with a narrow size distribution were synthesized, having an average particles size of 87 nm, as shown in Fig. 1b. When the silver precursor was heated in air, silver particles with an average size of 155 nm and wide size distribution were synthesized, as shown in Fig. 1c. To disclose the size effect of silver catalysts, silver catalysts synthesized were evaluated for ethylene epoxidation. We measured the selectivity of ethylene epoxidation at the same reactant conversion (2 % of ethylene conversion in all measurements). In the process of ethylene epoxidation, the partial pressure of ethylene was 0.1 and the O_2/C_2H_4 ratio was kept at 0.25 for all experiments and the balance was made up by N_2. The selectivity of the silver particles prepared in nitrogen was 80.24 % for ethylene epoxidation in the beginning. With the increase in reaction time, the selectivity decreased gradually, and finally reached a steady selectivity of 78.75 %. The selectivity of the catalysts prepared in air atmosphere was 77.46 %, and the average selectivity was 1.75 % lower than the catalysts prepared in nitrogen atmosphere.

To disclose the size dependent selectivity of silver catalysts, XRD was used to determine the crystal structure of silver particles, as shown in Fig. 2. No matter which kinds of atmospheres were used in the preparation of silver catalysts, crystalline silver particles as well as the alumina crystals were detected, as shown in Fig. 2a. Two silver catalysts have similar peaks. The peaks at 38.1° and 44.3° belong to the (1 1 1) and (2 0 0), respectively. When

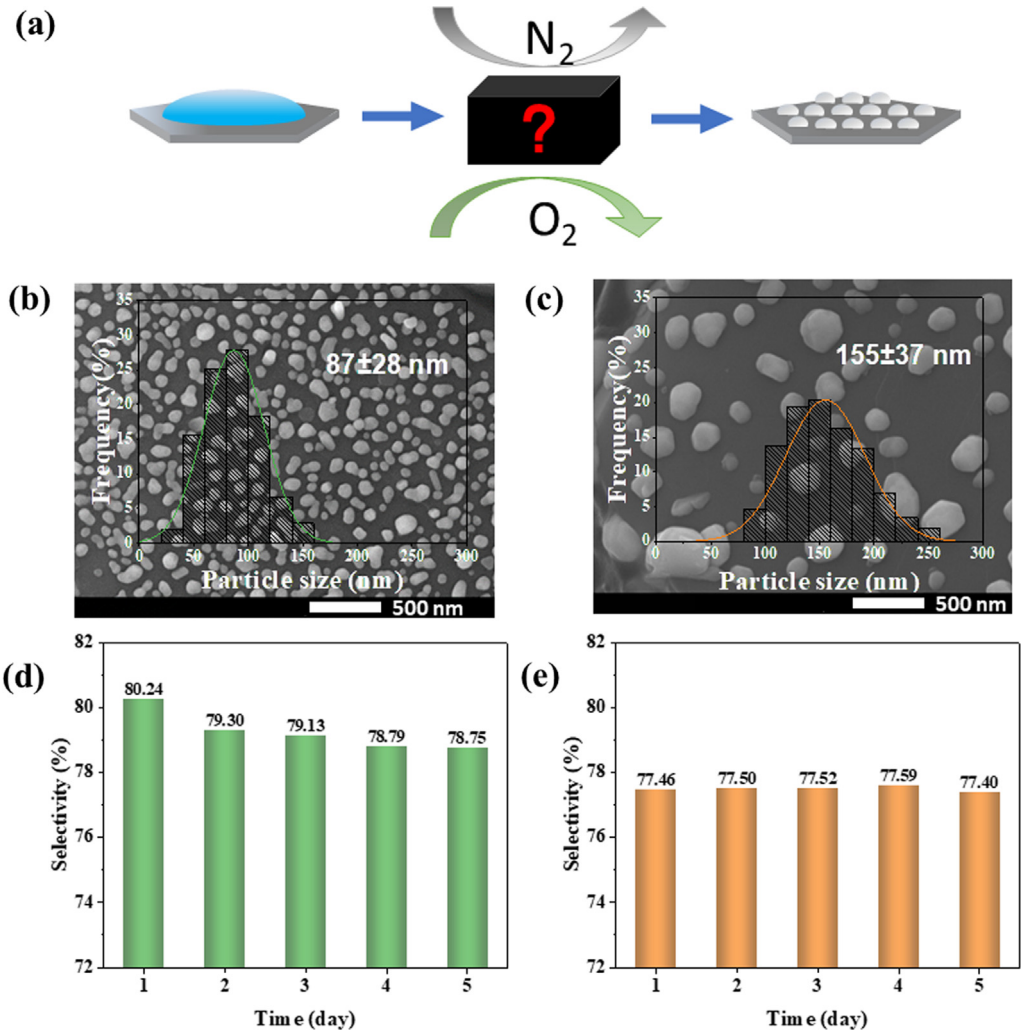

Fig. 1. An illustration of the thermal decomposition of silver precursor to form silver catalysts in which the atmosphere may play an important role (a). SEM images of silver catalysts prepared in nitrogen (b) and air (c) atmosphere. Inserts: particle size distribution of silver catalysts prepared. The selectivity of ethylene oxidation catalyzed by silver particles prepared in nitrogen (d) and air (e) atmosphere.

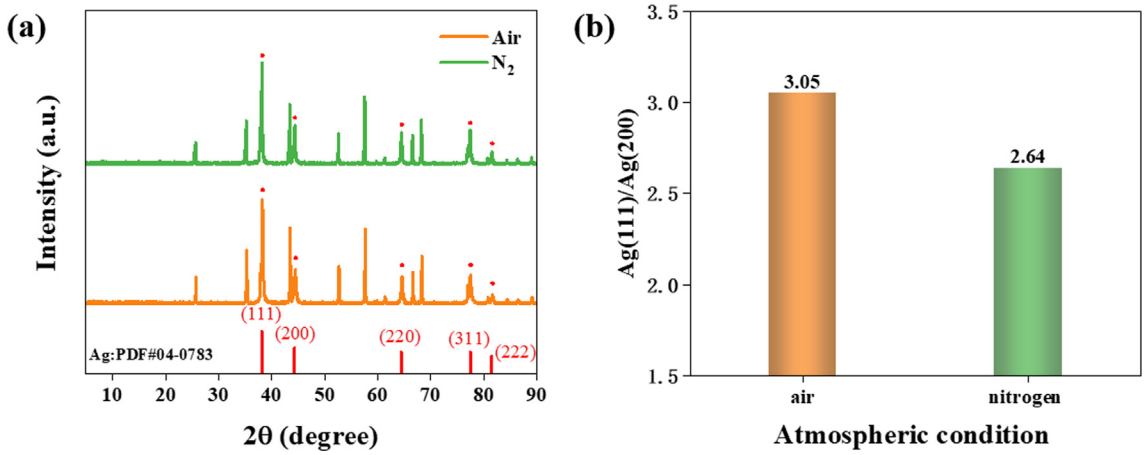

Fig. 2. XRD patterns of silver catalysts on alumina wafer after the thermal decomposition of silver precursors in air and nitrogen atmospheres (a). The ratio of Ag(1 1 1) to Ag (2 0 0) peak intensities synthesized at different atmospheric conditions.

we calculated the ratio of peaks intensity between Ag (1 1 1) and Ag (2 0 0), a difference was found. Silver catalysts prepared in nitrogen had a lower ratio, as shown in Fig. 2b, which was attributed to the higher intensity of (2 0 0) intensity in this sample than that prepared in air. Therefore, silver particle synthesized in nitrogen had more (2 0 0) facets exposed. Since the activation barriers of Ag (2 0 0) to form ethylene oxide are lower than Ag(1 1 1) [15,16], these small particles showed higher selectivity in ethylene epoxidation, which agreed well with previous investigations from other groups [15,16].

To disclose the formation process of silver catalysts, we employed CLSM equipped with a heating stage to *in-situ* observe the thermal decomposition of silver precursor, as shown in the videos of supporting information. Parts of the video were picked up and shown in Fig. 3. With the increase of temperature, the evaporation of water resulted in the crystallization of silver salts, as shown in Fig. 3b, followed by the decomposition of silver salts (Fig. 3c and 3d), forming silver particles at the surface of alumina wafer. To disclose this decomposition process, TG-DTA measurements were conducted. TG curves were shown in Fig. 4, and the DTA curves were shown in Figure S3. According to the TG curves, two rapid decreases of samples weight were found during the heating process. One was around 60 °C and the other was around

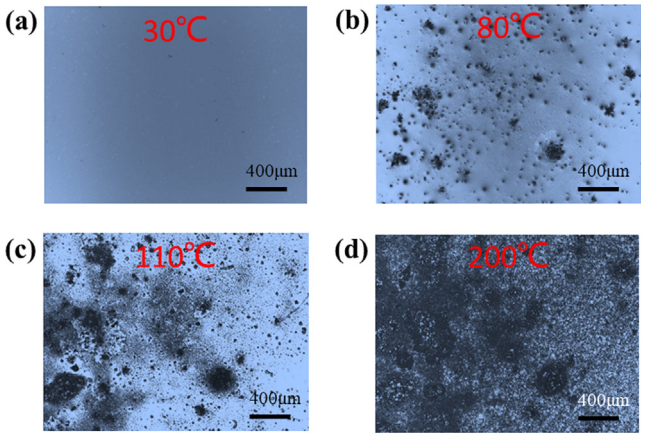

Fig. 3. Images of the decomposition process of silver precursors at different temperatures. These images were cut from the videos taken by confocal laser scanning microscopy.

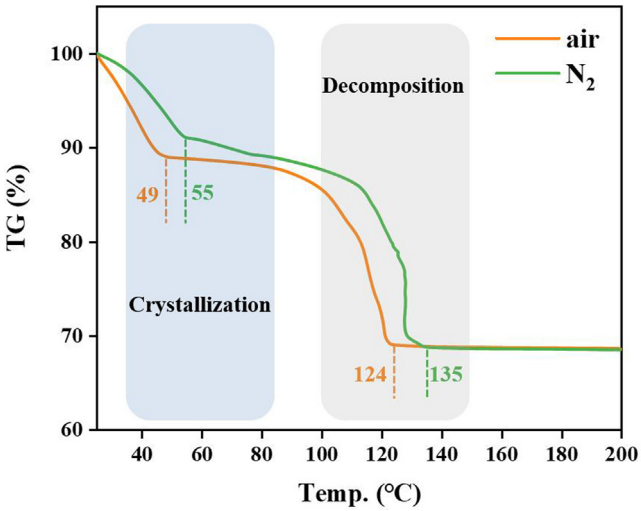

Fig. 4. TG curves of silver catalysts prepared in different atmospheres.

120 °C. The whole decomposition process could be divided into two stages: (1) crystallization process from room temperature to 80 °C, the weight loss in this process was contributed by the evaporation of solvents; (2) the decomposition process from 80 °C to 150 °C, during which the weight loss was attributed to the decomposition of the silver salt precursor to form silver particles. When the silver precursor was heated in air, the weight loss given by crystallization stopped at 49 °C, which was lower than that in nitrogen, as shown in Fig. 4. In the decomposition process, the weight loss stopped at 124 °C in air while the weight decreased until 135 °C in nitrogen. Both the crystallization and decomposition processes occurred at a lower temperature in air than that in nitrogen. The following study would attempt to reveal this difference.

To reveal the influence of the thermal atmosphere on the crystallization of silver complex, both the gas and solid products generated in the heating process at 30–70 °C were collected and characterized by different instruments, as shown in Fig. 5. The gas products were sent to the online MS attached to the TG-DTA. Water molecules were detected as the main products, as shown in Fig. 5b–c. In Fig. 5b, the signal of water molecules decreased gradually with temperature, indicating steady evaporation of water in nitrogen. In Fig. 5c, a peak of water signal was detected

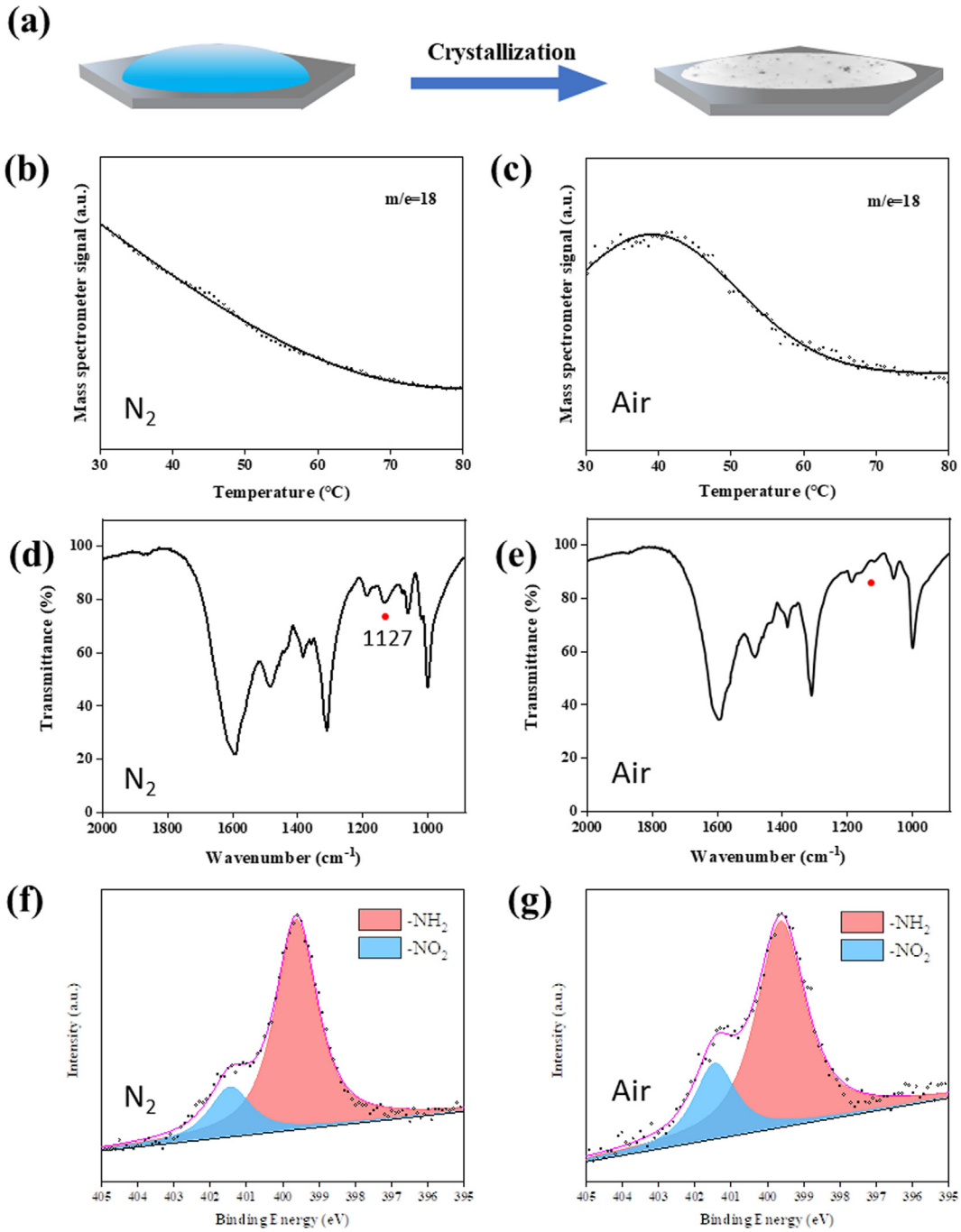

Fig. 5. Schematic diagram of the crystallization process in heating silver precursor on alumina wafer (a). Mass spectrum of H_2O (m/e = 18) released from the precursor in the nitrogen (b) and air (c) atmosphere. The infrared spectrum of crystals prepared in nitrogen (d) and air (e) atmosphere. The N_{1s} binding energy of crystals prepared in nitrogen (f) and air (g) atmosphere.

at 30–50 °C, indicating a quick evaporation of water in air. The solid products were characterized by FT-IR and XPS, as shown in Fig. 5d–g. When the silver precursor was heated in air, the absorption peak at 1127 cm^{-1} disappeared, as shown in Fig. 5e, which indicates the broken of long chain complex since the missing peaks were assigned to the C—N stretching vibrations of long chain amines [30]. These results suggested that the silver complex assembled by ethylenediamine and silver ions was destroyed by oxygen during the heating process, resulting in the formation of short chain complex. This hypothesis was supported by XPS. The solid samples heated in air had a higher amount of nitro groups (—NO_2) than that in nitrogen. The nitro groups accounted for 26.42 % of the total *N*-containing function groups for the samples heated in air while it was only 19.02 % for the samples heated in nitrogen, as shown in Fig. 5f and 5 g. The peak position of nitro groups and amino groups were consistent with the references. [31,32] The increase of nitro groups was ascribed to the reaction of silver complex with oxygen, as illustrated in Fig. S4. Furthermore, the broken long chain complex liberated the water adsorbed in molecules, which resulted in the quick evaporation of water in air, as shown in Fig. 5c. These results confirmed that the atmosphere influences the evaporation process as well as the solid intermediate, which may affect the structures of silver particles formed in the following heating process.

The solid products formed at 80 °C were further heated to 200 °C in different atmospheres to reveal the effect of thermal atmospheres on the silver catalysts, as shown in Fig. 6. In the decomposition process, oxalate groups were decomposed to reduce silver ions forming silver particles. Fig. 6b and 6c are the DTA curves of the precursor decomposition in different atmospheres. When the samples were heated in nitrogen, the endothermic peak occurred at 125 °C while it decreased to 120 °C in air, as shown in Fig. 6b and c. The decrease in decomposition temperature could be ascribed to the oxidation of ethylenediamine in air to destroy the long chain complex structure, forming short chain complex. The MS data in Fig. 6d and 6e showed that carbon dioxide was produced during the heating process, confirming the decomposition of oxalate in this stage. When the sample was heated in nitrogen, the decomposition occurred at the temperature from 102 °C to 130 °C, as shown in Fig. 6d, which resulted in the nucleation of silver particles followed by their growth, forming relatively similar size of particles, as shown in Fig. 6f. When the sample was heated in air, carbon dioxide was detected at 90 °C, as shown in Fig. 6e, indicating that the oxalate began to decompose at a relatively low temperature. The decomposition process lasted for a wide range of temperatures from 90 °C to 130 °C, in which the silver ions were continuously reduced, leading to a long-term crystallization of silver particles. The later nuclei attached to the initial silver particles, forming big particles with rough surface, as shown in Fig. 6g. Therefore, the thermal atmosphere plays an important role in the formation of silver catalysts, and a choice of the atmosphere may lead to the improvement of catalysts structure and performance.

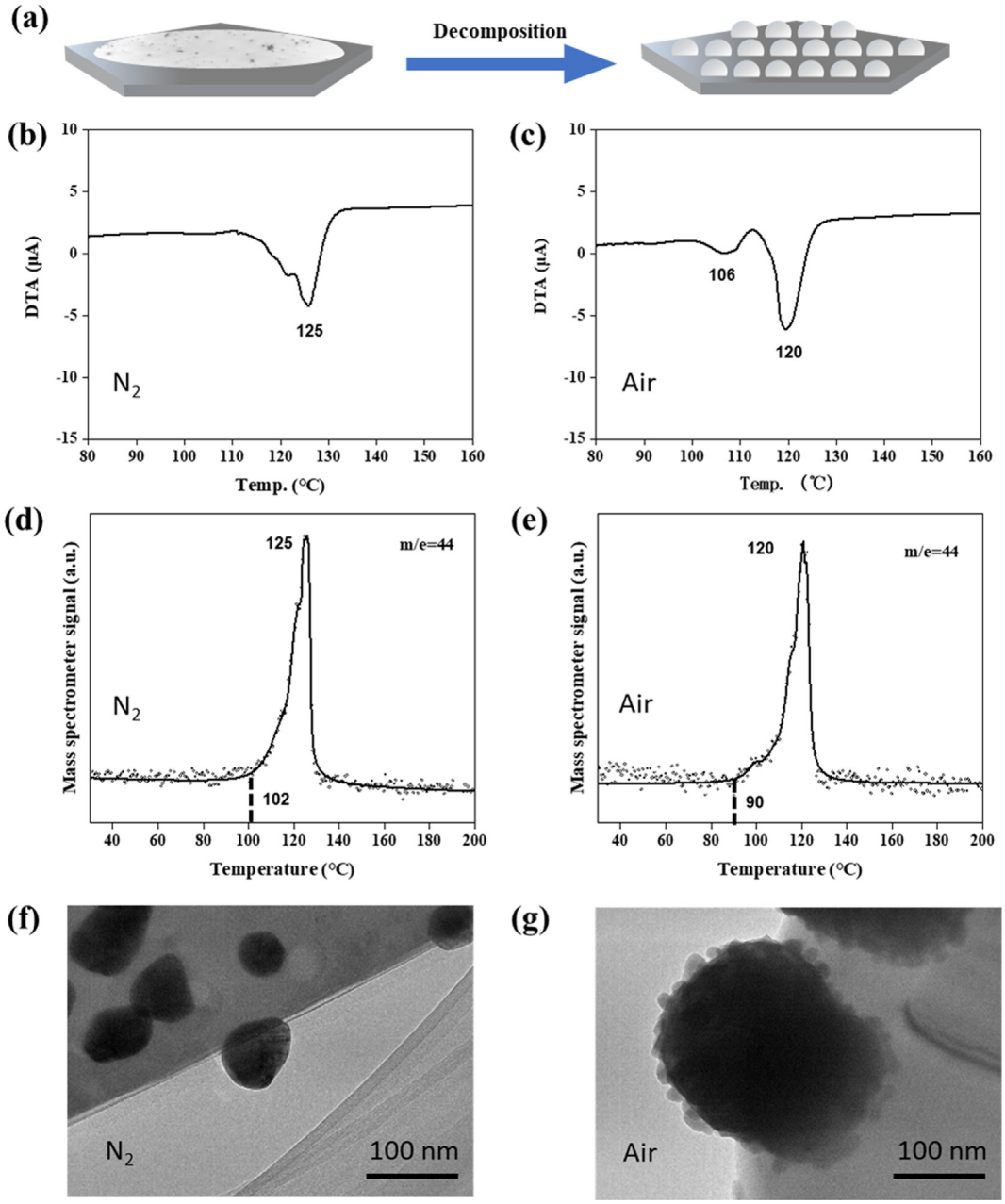

Fig. 6. Schematic diagram of the thermal decomposition of silver complex to form silver particles at alumina wafer (a). DTA curves of silver precursor decomposition in nitrogen (b) and air (c) atmosphere. Mass spectrum of CO_2 (m/e = 44) released from the precursor in the nitrogen (d) and air (e) atmosphere. TEM images of silver catalysts prepared in nitrogen (d) and air (g) atmosphere.

4. Conclusions

The thermal decomposition process of silver precursor to form silver catalysts was investigated by CLSM equipped with a heating stage. The formation of silver catalysts was disclosed into two steps, namely crystallization and decomposition. The crystallization process occurred below 80 °C, in which water was evaporated and solid products consisting of ethylenediamine, silver oxalate and bound water precipitated. The decomposition process took place at 90 to 140 °C, during which the decomposition of oxalate was accompanied by the formation of silver particles. It was found that thermal atmospheres played an important role in the formation of silver catalysts. When the silver precursor was heated in air, the oxygen attacked the silver complex formed in the crystallization process, leading to a low decomposition temperature and a long-term crystallization of silver particles, forming big silver particles with inhomogeneous size distribution. When the samples were heated in nitrogen, small silver particles with relatively similar sizes were generated, which led to a high selectivity of ethylene epoxidation when these particles were used as the catalysts. Therefore, a choice of thermal atmosphere promises a facile strategy to improve the structure and property of thermally decomposed catalysts.

Declaration of Competing Interest

The authors declare that they have no known competing financial interests or personal relationships that could have appeared to influence the work reported in this paper.

Acknowledgements

This work was supported by the National Natural Science Foundation of China (91934302, 21978298, U1862117), and the project from the State Key Laboratory of Multiphase Complex Systems (MPCS-2021-A-05).

Appendix A. Supplementary material

Supplementary data to this article can be found online at https://doi.org/10.1016/j.apt.2022.103732.

References

[1] J.T. Jankowiak, M.A. Barteau, Ethylene epoxidation over silver and copper-silver bimetallic catalysts: I. kinetics and selectivity, J. Catal. 236 (2) (2005) 366–378.
[2] M.O. Ozbek, I. Onal, R.A. van Santen, Why silver is the unique catalyst for ethylene epoxidation, J. Catal. 284 (2) (2011) 230–235.
[3] G. Boskovic, D. Wolf, A. Brückner, M. Baerns, Deactivation of a commercial catalyst in the epoxidation of ethylene to ethylene oxide-basis for accelerated testing, J. Catal. 224 (1) (2004) 187–196.
[4] A. Talati, M. Haghighi, F. Rahmani, Oxidative dehydrogenation of ethane to ethylene by carbon dioxide over Cr/TiO_2-ZrO_2 nanocatalyst: effect of active phase and support composition on catalytic properties and performance, Adv. Powder Technol. 27 (4) (2016) 1195–1206.
[5] A. Kakalj, P. Gava, S. de Gironcoli, S. Baroni, What determines the catalyst's selectivity in the ethylene epoxidation reaction, J. Catal. 254 (2) (2008) 304–309.
[6] E. Alp, E.C. Araz, A.F. Buluc, Y. Guner, Y. Deger, H. Esgin, K.B. Dermenci, M.K. Kazmanli, S. Truan, A. Genc, Mesoporous nanocrystalline ZnO microspheres by ethylene glycol mediated thermal decomposition, Adv. Powder Technol. 29 (12) (2019) 3455–3461.
[7] J.H. Miller, A. Joshi, X.Y. Li, A. Bhan, Catalytic degradation of ethylene oxide over Ag/α-Al_2O_3, J. Catal. 389 (2020) 714–720.
[8] J.E. van den Reijen, W.C. Versluis, S. Kanungo, M.F. d'Angelo, K.P. de Jong, P.E. de Jongh, From qualitative to quantitative understanding of support effects on the selectivity in silver catalyzed ethylene epoxidation, Catal. Today 338 (2019) 31–39.
[9] J.C. Dellamorte, J. Lauterbach, M.A. Barteau, Rhenium promotion of Ag and Cu-Ag bimetallic catalysts for ethylene epoxidation, Catal. Today 120 (2) (2007) 182–185.
[10] S. Linic, M.A. Barteau, On the mechanism of Cs promotion in ethylene epoxidation on Ag, J. Am. Chem. Soc. 126 (26) (2004) 8086–8087.
[11] E.J. Marek, S. Gabra, J.S. Dennis, S.A. Scott, High selectivity epoxidation of ethylene in chemical looping setup, Appl. Catal., B 262 (2020) 118216.
[12] S. Thakur, S. Singh, B. Pal, Time-dependent growth of CaO nano flowers from egg shells exhibit improved adsorption and catalytic activity, Adv. Powder Technol. 32 (9) (2021) 3288–3296.
[13] T.S. Ahmadi, Z.L. Wang, T.C. Green, A. Henglein, M.A. Elsayed, Shape-controlled synthesis of colloidal platinum nanoparticles, Science 272 (5270) (1996) 1924–1926.
[14] H.L. Wang, C.Y. Hsu, K.C.W. Wu, Y.F. Lin, D.H. Tsai, Functional nanostructured materials: aerosol, aerogel, and de novo synthesis to emerging energy and environmental applications, Adv. Powder Technol. 31 (1) (2020) 104–120.
[15] P. Christopher, S. Linic, Engineering selectivity in heterogeneous catalysis: Ag nanowires as selective ethylene epoxidation catalysts, J. Am. Chem. Soc. 130 (34) (2008) 11264.
[16] P. Christopher, S. Linic, Shape- and size- specific chemistry of Ag nanostructures in catalytic ethylene epoxidation, ChemCatChem 2 (1) (2010) 78–83.
[17] S.S. Sangaru, H.B. Zhu, D.C. Rosenfeld, A.K. Samal, D. Anjum, J.M. Basset, Surface composition of silver nanocubes and their influence on morphological stabilization and catalytic performance in ethylene epoxidation, ACS Appl. Mater. Interfaces 7 (51) (2015) 28576–28584.
[18] Y. Fu, Y. Ni, W. Cui, X. Fang, Z. Chen, Z. Liu, W. Zhu, Z. Liu, Insights into the size effect of $ZnCr_2O_4$ spinel oxide in composite catalysts for conversion of syngas to aromatics, Green Energy Environ. (2021), https://doi.org/10.1016/j.gee.2021.07.003.
[19] W.L. Gu, L.Y. Hu, C.S. Shang, J. Li, E.K. Wang, Enhancement of the hydrogen evolution performance by finely tuning the morphology of Co-based catalyst without changing chemical composition, Nano Res. 12 (1) (2019) 191–196.
[20] Y. Wang, Y.M. Qi, M.H. Fan, B.J. Wang, L.X. Ling, R.G. Zhang, C_2H_2 semi-hydrogenation on the Pd_xM_y cluster/graphdiyne catalysts: effects of cluster composition and size on the activity and selectivity, Green Energy Environ. 7 (3) (2022) 500–511.
[21] Z. Wang, G.A. Solan, Y.P. Ma, Q.B. Liu, T.L. Liang, W.H. Sun, Fusing carbocycles of inequivalent ring size to a bis(imino)pyridine-iron ethylene polymerization catalyst: distinctive effects on activity, PE molecular weight, and dispersity, Research 2019 (2019) 9426063.
[22] S.N. Goncharova, E.A. Paukshtis, B.S. Balzhinimaev, Size effects in ethylene oxidation on silver catalysts. Influence of support and Cs promoter, Appl. Catal., A 126 (1) (1995) 67–84.
[23] A.J.F. van Hoof, I.A.W. Filot, H. Fridrich, E.J.M. Hensen, Reversible restructuring of silver particles during ethylene epoxidation, ACS Catal. 8 (12) (2018) 11794–11800.
[24] A.J.F. van Hoof, E.A.R. Hermans, A.P. van Bavel, H. Fridrich, E.J.M. Hensen, Structure sensitivity of silver-catalyzed ethylene epoxidation, ACS Catal. 9 (11) (2019) 9829–9839.
[25] X.E. Verykios, F.P. Stein, R.W. Coughlin, Oxidation of ethylene over silver: adsorption, kinetics, catalyst, Catal. Rev.: Sci. Eng. 22 (2) (1980) 197–234.
[26] V.I. Bukhtiyarov, A.F. Carley, L.A. Dollard, M.W. Roberts, XPS study of adsorption on supported silver: effect of particle size, Surf. Sci. 381 (2–3) (1997) L605–L608.
[27] J.E. van den Reijen, S. Kanungo, T.A.J. Welling, M. Versluijs-Helder, T.A. Nijhuis, K.P. de Jongh, Preparation and particle size effects of Ag/α-Al_2O_3 catalysts for ethylene, J. Catal. 356 (2017) 65–74.
[28] X.H. Sun, S. Sartipi, F. Kapteijn, J. Gascon, Effect of pretreatment atmosphere on the activity and selectivity of Co/mesoHZSM-5 for Fischer-Tropsch synthesis, New J. Chem. 40 (5) (2016) 4167–4177.
[29] H. Wang, K. Lian, H.J. Wei, CN 111939884 A, 2020.
[30] X. Tao, L.S. Shi, M.J. Sun, N. Li, Synthesis of lignin amine asphalt emulsifier and its investigation by online FTIR spectrophotometry, Adv. Mater. Res. 909 (2014) 72–76.
[31] Z. Phiri, R.C. Everson, H.W.J.P. Neomagus, B.J. Wood, The effect of acid demineralising bituminous coals and de-ashing the respective chars on nitrogen functional forms, J. Anal. Appl. Pyrolysis 125 (2017) 127–135.
[32] N. Graf, A. Lippitz, T. Gross, F. Pippig, A. Hollander, W.E.S. Unger, Determination of accessible amino groups on surfaces by chemical derivatization with 3,5-bis (trifluoromethyl)phenyl isothiocyanate and XPS/NEXAFS analysis, Anal. Bioanal. Chem. 396 (2) (2010) 725–738.